ACS APPLIED ENERGY MATERIALS
Cite This: ACS Appl. Energy Mater. 2019, 2, 4135−4143
Article
www.acsaem.org

Spatial Molecular Layer Deposition of Ultrathin Polyamide To Stabilize Silicon Anodes in Lithium-Ion Batteries

Jasmine M. Wallas,[†] Brian C. Welch,[‡] Yikai Wang,[§] Jun Liu,[∥] Simon E. Hafner,[‡] Rui Qiao,[⊥] Taeho Yoon,[#] Yang-Tse Cheng,[§] Steven M. George,[†] and Chunmei Ban*[,⊥]

[†]Department of Chemistry and [‡]Department of Mechanical Engineering, University of Colorado, Boulder, Colorado 80309, United States
[§]Department of Chemical and Materials Engineering, University of Kentucky, Lexington, Kentucky 40506, United States
[∥]National Renewable Energy Laboratory, Golden, Colorado 80401, United States
[⊥]Department of Mechanical Engineering, Virginia Polytechnic Institute and State University, Blacksburg, Virginia 24060, United States
[#]School of Chemical Engineering, Yeungnam University, Gyeongsan 38541, Republic of Korea

Supporting Information

ABSTRACT: Cycling stability is central to implementing silicon (Si) anodes in next-generation high-energy lithium-ion batteries. However, challenges remain due to the lack of effective strategies to enhance the structural integrity of the anode during electrochemical cycling. Here, we develop a nanoscale polyamide coating, using spatial molecular layer deposition (MLD) of *m*-phenylenediamine and trimesoyl chloride precursors, to preserve the structural integrity of Si anodes. Poly(acrylic acid) (PAA) has been widely used in Si-based anodes as a binding agent due to its effective binding interactions with Si particles. However, the structural integrity of the anode is compromised by thermochemical decomposition of the poly(acrylic acid) binder, which can occur during electrode drying or during electrochemical cycling. Decomposition causes a 62% decrease in the elastic modulus of the Si anode, as measured by nanoindentation in electrolyte-soaked conditions. This study shows that an ultrathin polyamide coating counteracts this structural degradation, increases the elastic modulus of the degraded anode by 345%, and improves cohesion. Electrochemical analysis of polyamide-coated anodes reveals a film thickness dependence in cycling behavior. High overpotentials and fast capacity fading are observed for Si anodes with a 15 nm coating, whereas Si anodes with a 0.5 nm coating demonstrate stable cycling over 150 cycles with a capacity >1400 mAh g^{-1}. Our findings identify polyamide as an effective electrode coating material to enhance structural integrity, leading to excellent cyclability with higher capacity retention. Furthermore, the use of the spatial MLD approach to deposit the coating enables short deposition time and a facile route to scale-up.

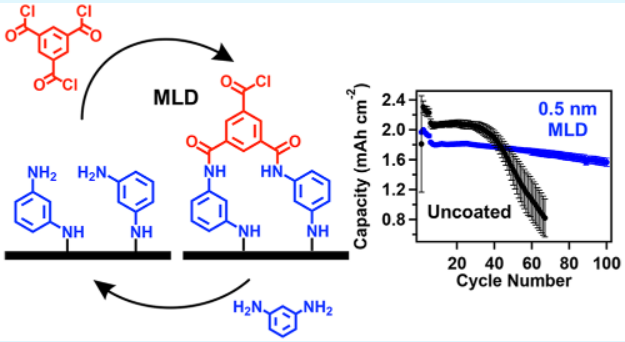

KEYWORDS: *molecular layer deposition, surface modification, polyamide, silicon anodes, lithium-ion batteries*

I. INTRODUCTION

There is an ever-increasing demand for energy storage technology with higher energy density for transportation and grid-connected renewable energy systems. This demand has fueled research into high-energy-density electrode materials, such as silicon (Si). Silicon has an almost 10-fold higher theoretical energy density (3579 mAh g^{-1}) than the conventional graphite anode (372 mAh g^{-1}) used in today's lithium-ion (Li-ion) batteries. However, silicon suffers from a ∼300% volume expansion upon lithiation and an unstable solid−electrolyte interphase (SEI), leading to poor electrochemical cycling stability.[1−3] Because of silicon's favorable properties, much recent research has focused on addressing its inherent cycling instability.

One strategy to mitigate the detrimental effects of volume changes in Si uses functional polymer binders that can enhance the mechanical integrity of the electrode. Poly(vinylidene fluoride) (PVDF) is the conventional polymer binder used in commercially available Li-ion batteries. However, this binder is unable to accommodate the large volume changes in silicon anodes upon cycling. Recent work has identified alternative binders, such as carboxymethyl cellulose (CMC) and poly(acrylic acid) (PAA), that can improve electrochemical performance of Si anodes.[4,5] Along with the improved

Received: February 15, 2019
Accepted: May 3, 2019
Published: May 3, 2019

DOI: 10.1021/acsaem.9b00326
ACS Appl. Energy Mater. 2019, 2, 4135−4143

mechanical properties of these two binders, the −OH and −COOH groups in these polymers interact favorably with the silicon surface.[6−8] However, PAA undergoes a reduction reaction to form an anhydride at elevated temperatures, losing −COOH groups and altering its mechanical properties.[9−11] In a vacuum, this reaction begins at temperatures of ≥100°C,[9] but in the presence of Li-ion battery electrolyte this reaction begins at ∼55 °C, where the reaction is catalyzed by the decomposition products of $LiPF_6$.[10] The formation of the anhydride is a concern in this system because it can lead to poor mechanical properties and poor electrochemical cycling. Therefore, strategies are needed to mitigate these effects.[10,11]

Another strategy to enhance the mechanical integrity of Si anodes is to modify their mechanical properties and stabilize Si surfaces through surface modification. Much research has focused on hybrid organic−inorganic coatings deposited with molecular layer deposition (MLD). One of the key benefits of MLD is its ability to conformally deposit a uniform coating on all surfaces within a high-aspect-ratio material, such as an electrode. Aluminum alkoxide or "alucone" coatings deposited with MLD are flexible and robust. These coatings can enhance the mechanical properties of Si anodes and thereby enable electrode integrity, leading to significantly improved cycling performance.[12−15] However, there are concerns that these coatings can react with Li^+ causing Li^+ depletion in the cell.[16] There is also a concern that conventional MLD is a time-consuming and difficult process, where the low vapor pressure of the organic precursors can create challenges.

To address these issues that have arisen from previous efforts to stabilize Si with MLD, we developed a novel, all-organic polymer MLD coating for the Si anode using a fast deposition process. The coating developed in this work is an aromatic polyamide material. Aromatic polyamides are known for their excellent chemical and thermal stability, making them suitable for the harsh, corrosive environment of an electrochemical cell.[17] Additionally, aromatic polyamides have high tensile strength and wear resistance.[18] Polyamides have been used in Li-ion batteries as cathode coatings,[19] binders,[20] and separators.[21] The coating developed in this study restored the favorable mechanical properties in silicon anodes that can be lost when PAA degrades. Moreover, a spatial MLD design, based on separating the precursors in space rather than in time, has been used here to deposit the polyamide coating for Si anodes. In spatial MLD, the substrate moves between zones where each precursor is continuously supplied. Using the spatial design, we reduced MLD deposition time from several hours to minutes. By using an all-organic polyamide material and depositing it using a spatial design, we were able to bring silicon anode technology closer to viability.

II. EXPERIMENTAL METHODS

Electrode Fabrication. Silicon composite anodes were prepared via slurry casting of Si (Alfa Aesar, plasma synthesized, ≤50 nm), carbon black (Super P, Timcal), and PAA (M_v ∼ 450000, Sigma-Aldrich) with a weight ratio of 60, 20, and 20%, respectively, in 1-methyl-2-pyrrolidinone (NMP) (anhydrous, 99.5%, Sigma-Aldrich). The mixture was coated onto a copper foil and dried at 70 °C in air. Electrode sheets were used as is either heat treated at 150 °C or heat treated at 150 °C and also coated with an MLD film. Si active materials in the electrodes have an approximate mass loading of 0.9 mg cm^{-2}. The electrodes were punched to 14 mm diameter discs and dried at 95 °C overnight in a vacuum oven prior to coin cell assembly.

MLD Coating. MLD was used to deposit thin film coatings on silicon anodes. Deposition was performed in a custom-built spatial MLD system enclosed within a convection oven. The operation[22] and design[23] of this rotary drum system were previously described. The nitrogen purge gas (99.998%, Airgas) separating precursor dosing zones had a flow rate of 1000 sccm. The convection oven encasing the entire system allowed uniform heating to the targeted deposition temperature of 150 °C. Once loaded into the reactor, samples were heated overnight at the deposition temperature to reach thermal equilibrium with the system. Anode samples were mounted to the inner drum of the spatial MLD system using Kapton adhesive tape. Tape was applied to all sides of the copper foil upon which the anode was mounted to seal and prevent deposition on the backside of the copper foil. For thicknesses measurements, a reflective and flexible witness sample was added to each deposition. The witness was a PEN polymer film (75 μm thick) metalized with titanium (sputtered, 80 nm thick (ROWO Coating). Precursors for two separate MLD chemistries were mounted onto the system. One set of precursors was trimethylaluminum (TMA) (97%, Sigma-Aldrich) and glycerol (99.5%, Sigma-Aldrich) to produce a hybrid organic−inorganic aluminum alkoxide (alucone). The other set of precursors was *m*-phenylenediamine (mPD) (99%, Sigma-Aldrich) and trimesoyl chloride (TMC) (98%, Sigma-Aldrich) to produce an all-organic aromatic polyamide. The TMA resided outside the oven enclosure at room temperature, while the other precursors resided within the convection oven of the system. Each precursor was connected to the system by two bellows globe valves on either side of the bellows needle valve for metering flow. The precursor exposure time was defined by the rotation speed of the inner drum upon which the samples resided as it moved through precursor dosing zones. The two rotation speeds used in this work, 0.5 and 5 rpm, correspond to exposure times of 6 and 0.6 s.[24]

The MLD film thickness was measured on the witness PEN sample with spectroscopic ellipsometry (SE) (M-2000, J.A. Woollam Co., Inc.) SE measurements were performed over a spectral range of 240−1685 nm with 50°, 60°, and 70° incident angles. Data were modeled with CompleteEASE v.4.55 (J.A. Woollam Co., Inc.). A Cauchy model was used to measure alucone films. Polyamide films were modeled with two Gaussian oscillator curves with an anisotropic index difference in the *z*-axis.

Electrochemical Cycling. Standard 2032 half-coin cells with Li metal foil as counter and reference electrodes were used. Cells were assembled in an Ar-filled glovebox. The electrolyte was 1.2 M $LiPF_6$ in ethylene carbonate (EC) and diethyl carbonate (DEC) in 3:7 v/v. Fluorethylene carbonate (FEC) was used as an additive at a weight ratio of 10%. The separator was Celgard 2325. Electrochemical tests were conducted at room temperature using an Arbin 2000 and a Maccor 4000 battery test station. For each condition, cycling data were plotted as an average of three cells with standard errors.

Fourier Transform Infrared Spectroscopy (FTIR). Attenuated total reflectance (ATR) FTIR (Nicolet 6700, Thermo Scientific) spectra were collected with a liquid nitrogen cooled MCT/A detector. Spectra were averaged over 200 scans with a scan resolution of ∼1 cm^{-1}. MLD films for analysis were deposited on copper foils.

Mechanical Testing. Nanoindentation measurements were conducted using a Nanoindenter G200 (Agilent) inside an argon-filled glovebox. A depth-controlled mode was used with an indentation strain rate of 0.05 s^{-1}, a maximum depth of 1200 nm, and a 10 s holding at the maximum load. The maximum depth was less than one-tenth of the electrode thickness such that the substrate effect can be neglected. Before nanoindentation tests, thermal drift was calibrated to be <0.5 nm s^{-1}. Thermal drift calibrations (100 s) were conducted after unloading. The elastic modulus and hardness values were obtained based on the Oliver−Pharr method.[25] Environmental nanoindentation measurements under wet conditions, with the electrode immersed in the electrolyte, were performed with a liquid cell. The technical details of environmental nanoindentation measurements under wet conditions were previously described.[26] During the measurement, the indenter tip was submerged in the electrolyte. Therefore, the interaction between the indenter and the electrolyte does not influence the measurements. The electrolyte was replaced every 40 min to avoid any precipitation of ethylene

DOI: 10.1021/acsaem.9b00326
ACS Appl. Energy Mater. 2019, 2, 4135−4143

carbonate and $LiPF_6$ that might influence measurements. Reported modulus and hardness values, as well as their standard deviations, were obtained by averaging over at least ten measurements.

Scratch tests were conducted with a conical indenter (cone angle of 60° and tip radius of 5 μm) using a NanoTest Vantage system (Micro Materials Ltd.). A prescan was conducted with a constant load of 0.1 mN to probe the roughness and tilt of the samples for calibrating the scratch depth profiles. During scratch tests, a normal load was applied after 50 μm scanning (at the load of 0.1 mN) with a loading rate of 0.5 mN/s. The maximum load (F_{max}), scratch distance, and the scanning velocity are 120 mN, 3000 μm, and 10 μm/s, respectively. The scratch continued until F_{max} was reached at a scan distance of 2450 μm. We conducted five scratch tests in each sample to assess the reproducibility of the results.

STEM-EDS. Imaging was conducted with a Tecnai F20 TEM (FEI Company) at an acceleration voltage of 200 kV. The system was equipped with energy-dispersive X-ray spectrometry (EDS) for elemental analysis. Samples were prepared by scratching the anode surface with a Cu grid. Samples from electrochemically cycled anodes were prepared and loaded in an Ar-filled glovebox. A Gatan vacuum transfer holder was used to transfer these samples into the instrument to avoid moisture and air exposure.

III. RESULTS AND DISCUSSION

Polyacrylic Anhydride Formation. The reduction of PAA is a well-known reaction that occurs at elevated temperatures. Reduction occurs when carboxylic acid groups in the polymer undergo a condensation reaction to form polyacrylic anhydride and release H_2O, according to the reaction in Figure 1. In Li-ion battery electrodes, the formation

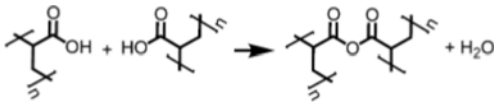

Figure 1. Reaction between carboxylic acid functional groups in poly(acrylic acid) occurs at elevated temperatures, producing polyacrylic anhydride and water.

of this anhydride from the PAA binder negatively affects battery performance.[10,11] This reaction reduces the number of carboxylic acid groups that can interact favorably with the hydroxyl groups on the silicon surface and weakens the adhesion between binders and Si particles, causing the electrochemical isolation of silicon and capacity fading of Si anodes. The anhydride reaction also causes polymer cross-linking, which decreases the elastic modulus of the binder and may reduce volume expansion compatibility.[11,27] Additionally, the water released upon anhydride formation can react with the electrolyte to form HF, which aggressively corrodes battery components.

Though this reaction usually occurs at elevated temperatures, it can also be catalyzed at lower temperatures by the decomposition products of the electrolyte. Under vacuum this reaction occurs at temperatures ≥100 °C.[9] However, when immersed in battery electrolyte, this reaction can occur at temperatures as low as 55 °C.[10] The formation of the anhydride can be monitored with FTIR. Figure S1 shows FTIR spectra of silicon composite electrodes, composed of silicon nanoparticles, PAA, and carbon black, dried under vacuum at different temperatures. Bands at ∼1710 and ∼1410 cm^{-1} indicate free carboxylic acid groups and bands at ∼1618 and 1455 cm^{-1} indicate hydrogen-bonded carboxylic dimers, all of which are characteristic of PAA. These peaks are prominent in the electrodes heat treated at 70 and 95 °C for ∼12 h and diminished in the electrode heat treated at 150 °C. In the electrode heated to 150 °C, the carboxylic anhydride peak is prominent, indicated by peaks at ∼1800 and ∼1012 cm^{-1}. Tests comparing cycling of electrodes after drying at 95 and 150 °C for ∼12 h are shown in Figure S2. Compared to the electrode heated to 95 °C, the electrodes heated to 150 °C show reduced galvanostatic cycling capacity.

Improving Anode Mechanical Properties with a Polyamide MLD Coating. In this work, a thin aromatic polyamide coating was used to enhance the structural integrity of the silicon composite electrode and counteract the negative effects of anhydride formation. The MLD coating was deposited via sequential, self-limiting surface reactions with the precursors *m*-phenylenediamine (mPD) and trimesoyl chloride (TMC). The proposed reaction mechanism for the deposition of this polyamide thin film is shown in Figure 2. A spatial MLD reactor design was used in these depositions. A detailed report on the spatial reactor used in these depositions was previously reported.[22] The coating was deposited directly onto the as-prepared electrodes. Because of the nanoscale features and high aspect ratio in the electrodes, long precursor exposure times were needed to deposit a conformal coating on all surfaces within the electrode.[24,28] Long exposure times present a challenge in the design of spatial ALD or MLD reactors. The precursor exposure times in this system were studied using the well-known MLD chemistry, alucone, deposited with the precursors trimethylaluminum and glycerol. A description of galvanostatic cycling of alucone-coated electrodes deposited with different exposure times is included in the Supporting Information (Figure S3). These tests indicated that the best electrochemical performance was realized with the longest exposure times studied, 6 s. The best polyamide MLD coating, with a thickness of 0.5 nm, was deposited with the 6 s exposure time.

The polyamide MLD coating has several favorable properties as a silicon electrode coating. Aromatic polyamides are generally considered chemically stable. To illustrate, a 354 nm MLD coating on Cu was soaked in electrolyte for 24 h. After soaking, the coating appeared unscathed. No significant mass change was observed after soaking. A large mass increase in the coating would be expected if it were to react strongly with electrolyte. Indeed, the FTIR spectra of this sample remained unchanged after soaking, suggesting that there was no appreciable chemical change in the material (Figure S4). Aromatic polyamides are also generally considered insoluble in organic solvents. The insolubility of the MLD coating increases the structural integrity of the electrode when immersed in organic solvent. Figure S5 shows electrodes soaked in NMP solvent for 48 h and then sonicated for 2 min. The pristine electrode completely dissolved in the solvent. The electrode that was heat treated at 150 °C, and therefore contained polyacrylic anhydride, showed partial solubility in the solvent. In comparison, an electrode coated with 0.5 nm of MLD was the most stable and was largely insoluble.

Polyamides also have favorable mechanical properties. Mechanical testing, shown in Figure 3, indicates that some of the negative effects of anhydride formation can be mitigated by coating the electrode with a very thin MLD coating. Nanoindentation measurements, shown in Figure 3A, were performed on electrodes under wet conditions to better mimic the electrolyte environment in batteries.[26] Compared to an electrode dried at 70 °C, an electrode dried at 150 °C had a lower elastic modulus but higher hardness. The elastic

DOI: 10.1021/acsaem.9b00326
ACS Appl. Energy Mater. 2019, 2, 4135−4143

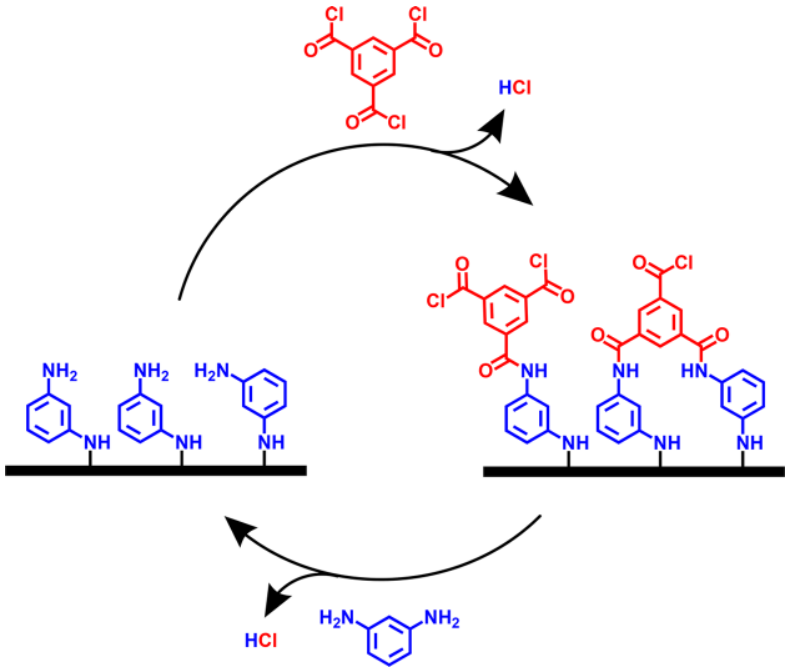

Figure 2. Reaction mechanism for the deposition of an aromatic polyamide thin film using the precursors trimesoyl chloride and *m*-phenylenediamine.

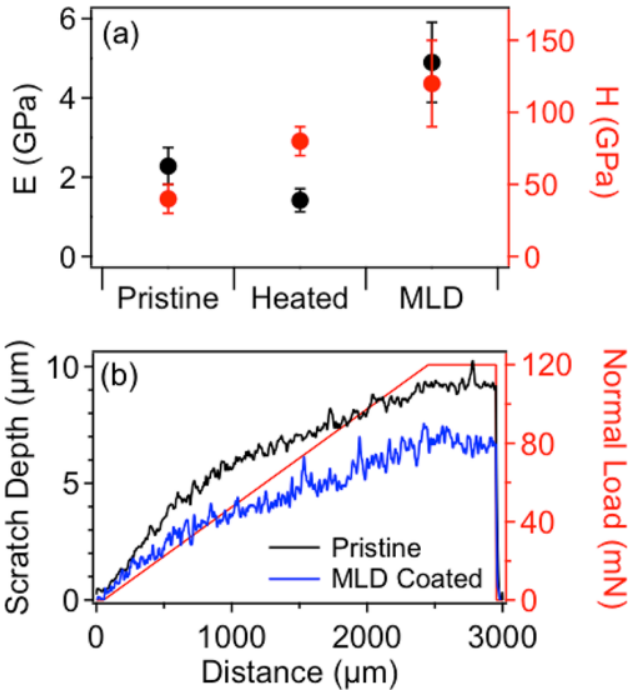

Figure 3. Mechanical testing of silicon composite electrodes before and after heating at 150 °C and with a 0.5 nm polyamide coating. (a) Elastic modulus and hardness values from nanoindentation under wet conditions, with electrodes soaked in electrolyte. After heating to 150 °C the elastic modulus of the electrode is reduced. However, with a polyamide coating this effect is mitigated. (b) Scratch testing indicates increased cohesion of the electrode coated with polyamide.

modulus was reduced by 62%, from 2.28 ± 0.47 to 1.42 ± 0.29 GPa. The MLD coating increased the elastic modulus of the electrode dried at 150 °C by 345% to 4.90 ± 1.01 GPa. The coating also increased the hardness by about 50%, from 0.08 ± 0.01 to 0.12 ± 0.03 GPa. The higher elastic modulus and hardness of the coated electrode indicate that the coating improves the mechanical properties of the electrode. Higher elastic modulus and hardness may make the electrode more resistant to the mechanical deformation and cracking associated with lithiation and delithiation of silicon.[29,30] The improved mechanical properties of the coated electrode may contribute to the improved electrochemical cycling stability of the MLD-coated electrodes described below.

We conducted scratch tests on the electrodes to investigate the influence of the MLD coating on the cohesion strength of Si electrodes. As shown in Figure 3B, the MLD-coated electrode had a smaller scratch depth under the same normal load and distance as compared to the uncoated one. The coated electrode also had a smaller scratch width compared to the uncoated electrode, as shown in Figure S6. The scratch resistance of the MLD-coated electrode indicates that it has a larger load-bearing capacity than the uncoated one. SEM images of the scratch tests, shown in Figure S6, show a distinct difference in scratch resistance between the coated and uncoated electrodes. The first 500 μm of scratch distance, scratched at a constant loading rate of 0.5 mN μm^{-1}, showed considerable electrode material detachment from the active layer of the uncoated electrode. In comparison, the coated electrode showed little electrode material detachment in the same distance and with the same loading rate. On the basis of these results, it is reasonable to infer that the MLD coating strengthens and improves the cohesion of the composite electrodes.

Extended Electrochemical Cycling of Polyamide-Coated Anodes. Enhancement in electrochemical performance of polyamide MLD-coated Si anodes was probed with galvanostatic cycling, as shown in Figure 4. Tests were conducted using a half-cell configuration with lithium metal as the counter electrode. All electrodes were heat treated to 150 °C for ~12 h and therefore contained polyacrylic

DOI: 10.1021/acsaem.9b00326
ACS Appl. Energy Mater. 2019, 2, 4135−4143

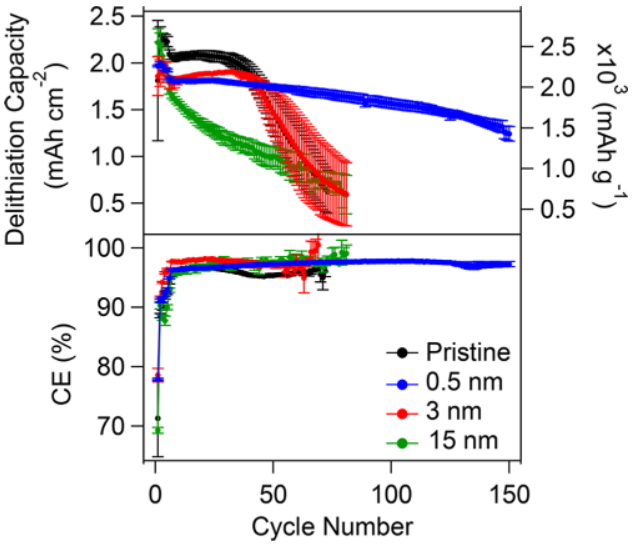

Figure 4. Galvanostatic discharge and charge cycling of pristine silicon composite electrodes compared to those coated with 0.5, 3, and 15 nm of polyamide showing extended capacity retention with a thin 0.5 nm polyamide coating. The first five cycles were run at a C/25 rate, and the following cycles were run at a C/10 rate. The 0.5 nm coating was deposited with long precursor exposure times, and the other two coatings were deposited with short precursor exposure times. For each condition, cycling data were plotted as the average of three cells with standard error bars.

anhydride. Electrochemical cycling performance of an uncoated, pristine electrode was compared with the MLD-coated electrodes with three different coating thicknesses. The three MLD coating thicknesses were 0.5, 3, and 15 nm, as measured with spectroscopic ellipsometry on Ti-coated PEN witness samples that were included in each deposition. Note that the 3 and 15 nm polyamide coatings were deposited with a 0.6 s exposure time, while the 0.5 nm coating was deposited with a 6 s exposure time. The coatings deposited with shorter exposure times may be less conformal than those deposited with longer exposure times, as discussed in the previous section and Figure S3. For the first five cycles, current was driven at a C/25 rate (143 mA g^{-1}), with the following cycles at a C/10 rate (358 mA g^{-1}). Electrodes were cycled between 0.010 and 1.000 V against a lithium−metal counter electrode, with a 10 min voltage hold at the lower cutoff voltage of 0.010 V and a 30 min voltage hold at 1.000 V.

Galvanostatic cycling behavior indicates a marked increase in performance when the Si electrode is coated with 0.5 nm of MLD polyamide. The pristine electrodes experienced a rapid capacity fade after ∼50 cycles and lost reversibility within 100 cycles. The electrodes coated with 3 nm of MLD showed favorable cycling performance in the first ∼50 cycles, but the capacity rapidly faded after that in a similar fashion to the uncoated electrode. The electrodes coated with 15 nm of MLD showed steady capacity fade beginning in the initial cycles. The electrodes coated with 0.5 nm of MLD demonstrated stable cycling over 150 cycles, with a capacity of 1427 ± 88 mAh g^{-1} at the 150th cycle. We did not measure electrochemical cycling past 150 cycles due to the known instability of Li metal[31,32], and marked a small increase in capacity variability approaching cycle 150. Between cycles 6 and 100, these cells cycled at ∼1.6 mAh cm^{-2}. At cycle 100, these cells retained 80% of their initial average capacity. The electrodes coated with 0.5 nm of MLD also maintained higher Coulombic efficiencies (CE) as compared to the pristine electrodes. Initial CE was low in both the coated and uncoated electrodes. The low CE in the first few cycles is likely a result of the high Si content in the electrodes. In the first few cycles, Si contributes to the lower CE through its phase transformations, side reactions, and SEI formation.[33,34] The 0.5 nm coated electrodes cycled with ∼97% efficiency between 10 and 150 cycles.

A comparison of voltage profiles among the coated and uncoated anodes, shown in Figure 5A, confirms that the electrochemical cycling performance of the anode is significantly improved with the ultrathin (0.5 nm) polyamide coating. During the first lithiation, the pristine anodes have voltage profiles with relatively flat voltage plateaus at ∼0.1 V vs Li/Li$^+$, which is consistent with the first lithiation of silicon particles at room temperature.[35] The first lithiation voltage profile of the 0.5 nm coated anodes has a similar voltage plateau at ∼0.1 V vs Li/Li$^+$. However, in contrast to the pristine anodes, the 0.5 nm polyamide coated anodes have less capacity for the first lithiation due to less capacity contribution above 0.3 V vs Li/Li$^+$. The polyamide coating can suppress detrimental side reactions that occur in the first electrochemical cycle due to its insulation properties and different surface chemistry.[36] In contrast, Si anodes with a thick coating (15 nm) have a distinct voltage profile for the first lithiation, with an inflection point at ∼0.5 V vs Li/Li$^+$ and a sloping voltage profile between ∼0.6 and ∼0.1 V vs Li/Li$^+$. The voltage dip at ∼0.5 V vs Li/Li$^+$ may indicate a kinetically limited step in the initial lithiation reaction, which has been seen in other systems with high overpotentials.[37,38] The slope between ∼0.5 and ∼0.1 V vs Li/Li$^+$ may be the result of absorption or chemical reaction of Li$^+$ at the surface of the polyamide coating.[20] The unusual behavior of the 15 nm coated electrode in the first cycle likely contributes to its higher capacity. However, as displayed in Figure S4, FTIR data suggest there is no observed interaction between the bulk polyamide coating and the electrolyte. After initial lithiation, the 15 nm coated anode shows typical lithiation and delithiation behavior. Further study is planned to investigate the reactivity of MLD polyamide materials within the electrochemical environment. The voltage profiles confirm the fast-fading electrochemical performances of both the pristine and the 15 nm coated Si anodes. The major contribution to capacity degradation of the pristine Si anode is likely the loss of electronic contact, a product of large volumetric changes upon cycling.[1−3]

The enhanced electrochemical reversibility in the 0.5 nm coated anodes is also illustrated in the differential capacity plots, as shown in Figure 5B. The differential capacity plots for both coated and uncoated electrodes indicate typical electrochemical behavior for Si anodes, including phase transformations between lithiated and delithiated phases.[39] The lithiation overpotential for the anode with a 0.5 nm polyamide coating is smaller and more stable than the pristine and 15 nm coated electrodes. At cycle 6, lithiation onset occurs at 0.55, 0.42, and 0.34 V vs Li/Li$^+$ for the 0.5 nm coated, pristine, and 15 nm coated electrodes, respectively. At cycle 10, lithiation onset occurs at 0.51, 0.37, and 0.27 V vs Li/Li$^+$ for the 0.5 nm coated, pristine, and 15 nm coated electrodes, respectively. At cycle 100, though the lithiation onset for the 0.5 nm coated electrode is 25 mV later than it was at cycle 6, the cells in the other conditions have reached failure. The increased overpotential seen in all three conditions is likely a product of increased contact resistance due to continual SEI formation.

DOI: 10.1021/acsaem.9b00326
ACS Appl. Energy Mater. 2019, 2, 4135−4143

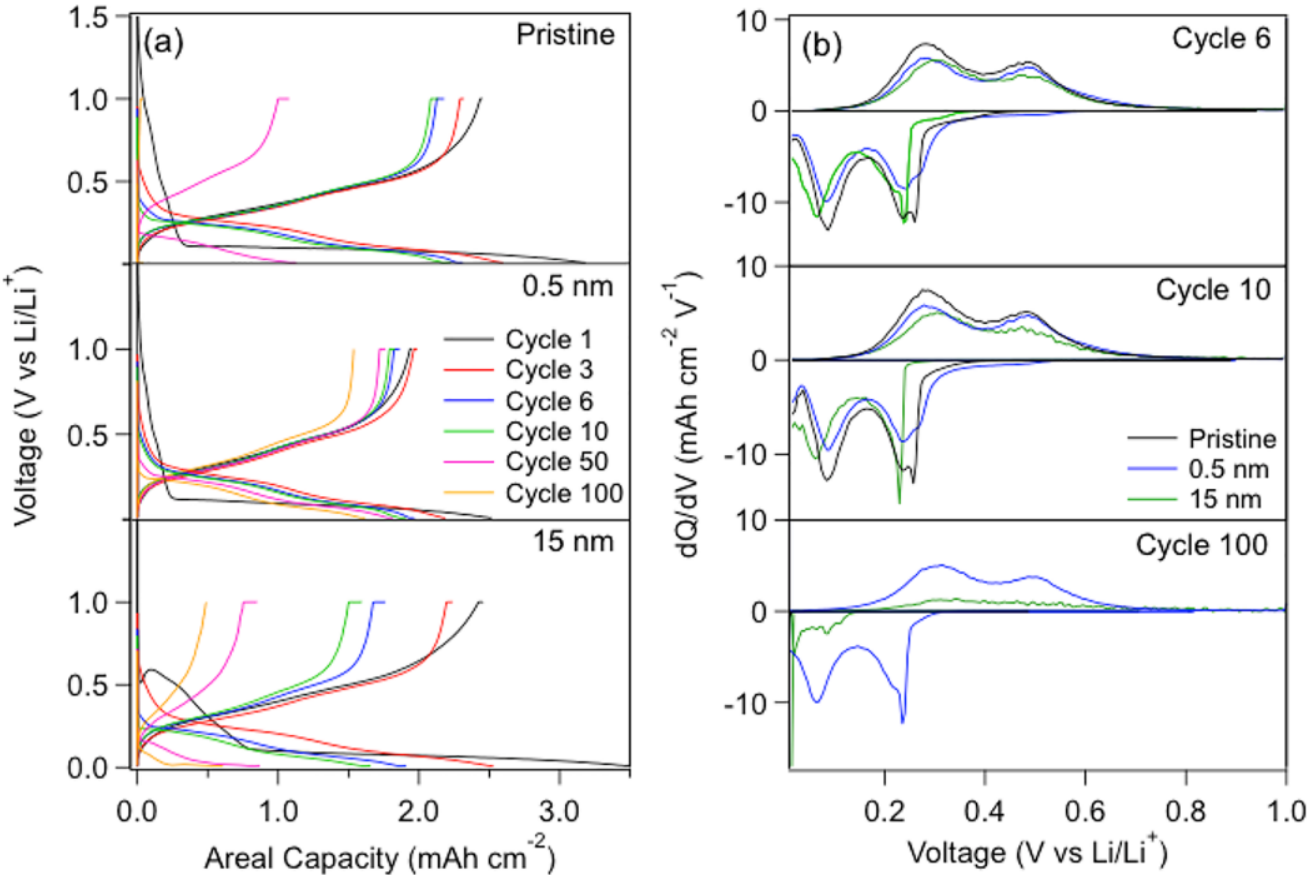

Figure 5. (a) Voltage profiles and (b) dQ/dV analysis of representative cells comparing cycling of pristine silicon composite electrodes compared to those coated with 0.5 and 15 nm of polyamide. The first five cycles were run at a C/25 rate, and the following cycles were run at a C/10 rate. Voltage fade and lithiation overpotential are mitigated by the 0.5 nm MLD coating and enhanced by the 15 nm MLD coating.

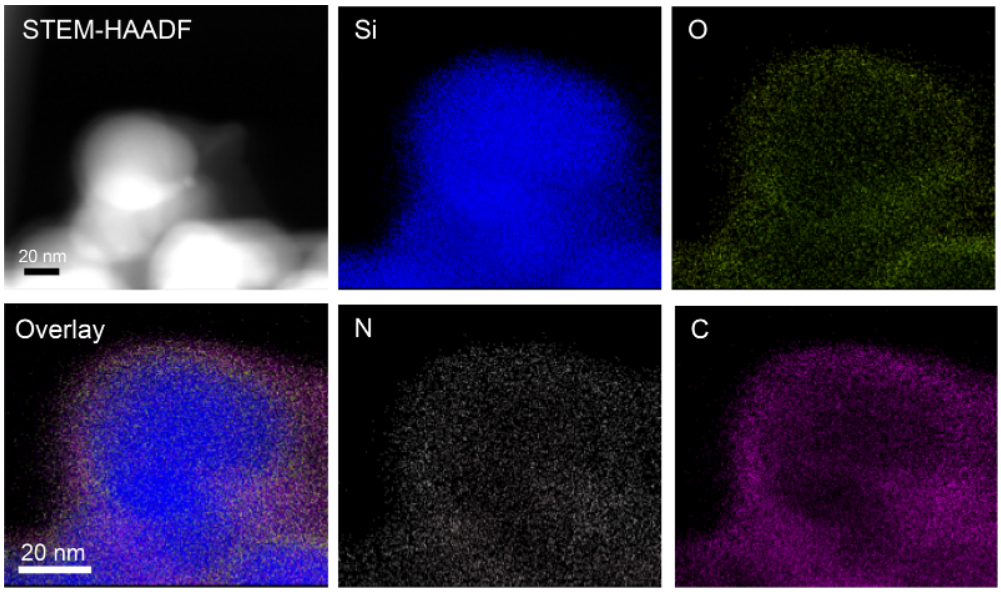

Figure 6. STEM-HAADF-EDS of silicon nanoparticles extracted from a silicon composite electrode coated with 15 nm of polyamide. Silicon nanoparticles appear uniform and spherical. The N signal is solely from the polyamide coating. Elemental mapping shows a uniform distribution of polyamide coating over the silicon nanoparticles.

However, the thin 0.5 nm MLD coating appears to largely mitigate overpotential effects with extended cycling as compared to the pristine electrode. There is a small but steady increase in overpotential in the cells with the 0.5 nm coated electrodes upon cycling. The increasing overpotential likely leads to an increase in incomplete delithiation upon cycling

DOI: 10.1021/acsaem.9b00326
ACS Appl. Energy Mater. 2019, 2, 4135−4143

and is likely the cause of the decreasing cycling capacity.[39] In comparison, the 15 nm MLD coating appears to increase overpotential effects, indicating that the thickness of the coating is critical to ensure cycling reversibility for Si anodes.

The poor cycling performance of the electrodes with thick MLD coatings illustrates the necessity of controlling the thickness of the coating. Because aromatic polyamides are well-known to be nonconductive,[40,41] thicker coatings may significantly increase the resistance in the cell. Indeed, there is clear evidence that MLD coatings can increase cell resistance.[15] While the thicker MLD coatings in this study had detrimental effects on electrochemical performance, the thinner MLD coating extended cycling capacity and reduced voltage fade. The coating may impart beneficial effects on electrochemical cycling by aiding mechanical integrity and by reducing potential side reactions through modification of the electrode surface.[36] However, these beneficial effects may be outweighed by the added resistance caused by the coating when thicker. The interplay between the advantageous and disadvantageous effects of the coating are clearly evident in electrochemical cycling of the electrodes coated with 3 nm of MLD, which showed favorable performance initially and then rapidly declined. It is possible that the added resistance from the MLD coating is minimized when the coating is very thin, allowing the advantageous effects to dominate.

Elemental Mapping of Polyamide-Coated Anodes. Figures 6 and 7 show the HAADF-STEM-EDS elemental mapping of silicon nanoparticles extracted from a 15 nm coated electrode before and after galvanostatic cycling, respectively. Before cycling, spherical silicon particles of ~50 nm in diameter are uniformly distributed. Elemental mapping shows the presence of silicon, oxygen, nitrogen, and carbon. The source of the oxygen signal may be from the native oxide on silicon, the carboxylic acid groups in PAA, and the amide groups in the MLD coating. The source of the carbon signal may be from carbon black or PAA. Only the nitrogen signal is solely indicative of the presence of the MLD coating. Though the nitrogen signal has a low intensity, elemental mapping in Figure 6 suggests that the coating is evenly dispersed and conformally coated over the entire silicon particle. After cycling, additional elemental signals are present as a result of exposure to the electrolyte and formation of the SEI, as shown in Figure 7. The additional elements present are phosphorus and fluorine, which are common species in the SEI layer of Si anodes. The silicon undergoes a morphology change from spherical nanoparticles to irregularly shaped particles after cycling. Elemental mapping reveals the continued presence of a nitrogen signal from the MLD coating on the cycled particles. Though the nitrogen signal is attenuated, likely a result of the formation of the SEI, the nitrogen signal appears to continue to overlap with the surface of the silicon particle. Furthermore, the STEM results indicate that the MLD polyamide coating may maintain intimate contact with the silicon particles during electrochemical cycling.

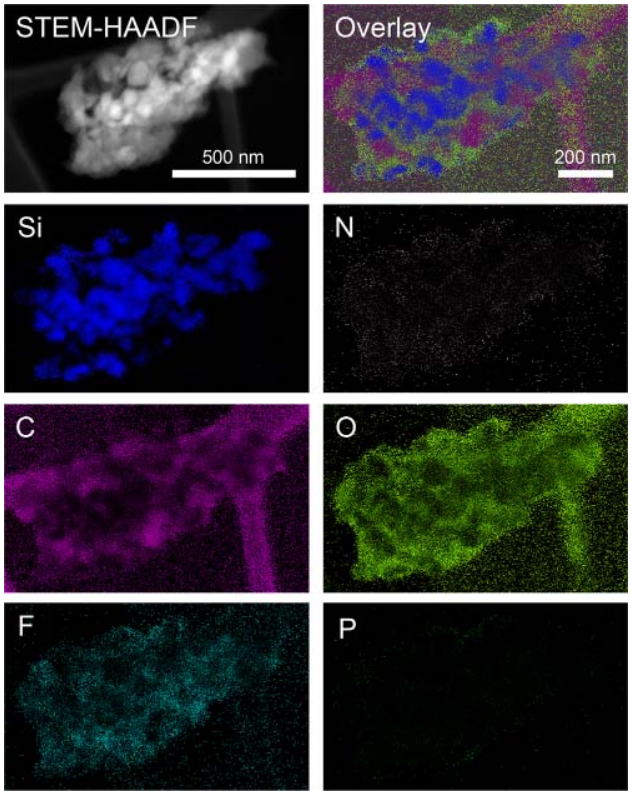

Figure 7. STEM-HAADF-EDS of silicon nanoparticles extracted from a silicon composite electrode initially coated with 15 nm of polyamide prior to electrochemical cycling. The Si particles show a distinct morphology change. Despite this morphology change, the nitrogen signal representative of the polyamide coating is still present in the area of the Si particles.

IV. CONCLUSIONS

The polyamide MLD coating developed in this work enables reversible cycling of Si anodes by improving its mechanical strength and structural integrity. This work examined the effect of an ultrathin polyamide coating on electrodes with thermally degraded PAA binder. With the ultrathin polyamide coating, the Si electrodes exhibit improved cohesion and the elastic modulus of the anode was increased by 345%. The coating imparts favorable mechanical properties to the Si anodes. We also examined the impact of the thickness of the coating on electrochemical cycling stability. While a 15 nm coating caused high overpotentials and rapid capacity fading, an ultrathin 0.5 nm coating enabled stable cycling over 150 cycles. Furthermore, the polyamide coating was deposited with a spatial MLD chamber, permitting fast deposition and a viable route to scale-up. The MLD coating explored in this work differs from previous studies of MLD coatings in three ways: (1) this MLD coating is an all-organic polymer and does not contain any metals, (2) this MLD coating is 5 times thinner than the alucone MLD coatings explored previously, and (3) the MLD coating was deposited with a spatial reactor. The mechanism that allows this thin coating to impart stable cycling is likely related to its increased elasticity, low solubility, and chemical resistance. Future work on this coating may use *in situ* techniques to examine the mechanisms responsible for the favorable properties of the MLD coating.

■ ASSOCIATED CONTENT

Supporting Information

The Supporting Information is available free of charge on the ACS Publications website at DOI: 10.1021/acsaem.9b00326.

FTIR spectra of silicon anodes at elevated temperatures, electrochemical cycling of uncoated anodes before and after heat treatment, electrochemical cycling of alucone-

DOI: 10.1021/acsaem.9b00326
ACS Appl. Energy Mater. 2019, 2, 4135−4143

coated anodes, FTIR spectra of PAA before and after electrochemical cycling, SEM images of scratch tests (PDF)

AUTHOR INFORMATION

Corresponding Author

*(C.B.) E-mail: chunmeiban@vt.edu.

ORCID

Jun Liu: 0000-0003-0159-9767

Rui Qiao: 0000-0001-5219-5530

Steven M. George: 0000-0003-0253-9184

Chunmei Ban: 0000-0002-1472-1496

Notes

The authors declare no competing financial interest.

ACKNOWLEDGMENTS

This work was authored in part by Alliance for Sustainable Energy, LLC, the manager and operator of the National Renewable Energy Laboratory for the U.S. Department of Energy (DOE) under Contract DE-AC36-08GO28308. The research is supported by the Vehicle Technologies Office of the U.S. Department of Energy Office of Energy Efficiency and Renewable Energy, under the supervision of David Howell, Brian Cunningham, and Peter Faguy. The authors also want to thank the startup grant from the Department of Mechanical Engineering at Virginia Tech.

REFERENCES

(1) Obrovac, M. N.; Krause, L. J. Reversible Cycling of Crystalline Silicon Powder. *J. Electrochem. Soc.* **2007**, *154* (2), A103.

(2) Chan, C. K.; Ruffo, R.; Hong, S. S.; Cui, Y. Surface Chemistry and Morphology of the Solid Electrolyte Interphase on Silicon Nanowire Lithium-Ion Battery Anodes. *J. Power Sources* **2009**, *189* (2), 1132−1140.

(3) Liu, X. H.; Zhong, L.; Huang, S.; Mao, S. X.; Zhu, T.; Huang, J. Y. Size-Dependent Fracture of Silicon Nanoparticles During Lithiation. *ACS Nano* **2012**, *6* (2), 1522−1531.

(4) Magasinski, A.; Zdyrko, B.; Kovalenko, I.; Hertzberg, B.; Burtovyy, R.; Huebner, C. F.; Fuller, T. F.; Luzinov, I.; Yushin, G. Toward Efficient Binders for Li-Ion Battery Si-Based Anodes: Polyacrylic Acid. *ACS Appl. Mater. Interfaces* **2010**, *2* (11), 3004−3010.

(5) Li, J.; Lewis, R. B.; Dahn, J. R. Sodium Carboxymethyl Cellulose. *Electrochem. Solid-State Lett.* **2007**, *10* (2), A17.

(6) Hochgatterer, N. S.; Schweiger, M. R.; Koller, S.; Raimann, P. R.; Wöhrle, T.; Wurm, C.; Winter, M. Silicon/Graphite Composite Electrodes for High-Capacity Anodes: Influence of Binder Chemistry on Cycling Stability. *Electrochem. Solid-State Lett.* **2008**, *11* (5), A76−A80.

(7) Munao, D.; van Erven, J. W. M.; Valvo, M.; Garcia-Tamayo, E.; Kelder, E. M. Role of the Binder on the Failure Mechanism of Si Nano-Composite Electrodes for Li-Ion Batteries. *J. Power Sources* **2011**, *196* (16), 6695−6702.

(8) Jeena, M. T.; Lee, J.-I.; Kim, S. H.; Kim, C.; Kim, J.-Y.; Park, S.; Ryu, J.-H. Multifunctional Molecular Design as an Efficient Polymeric Binder for Silicon Anodes in Lithium-Ion Batteries. *ACS Appl. Mater. Interfaces* **2014**, *6* (20), 18001−18007.

(9) McNeill, I. C.; Sadeghi, S. M. T. Thermal Stability and Degradation Mechanisms of Poly(Acrylic Acid) and Its Salts: Part 1—Poly(Acrylic Acid). *Polym. Degrad. Stab.* **1990**, *29* (2), 233−246.

(10) Nguyen, C. C.; Yoon, T.; Seo, D. M.; Guduru, P.; Lucht, B. L. Systematic Investigation of Binders for Silicon Anodes: Interactions of Binder with Silicon Particles and Electrolytes and Effects of Binders on Solid Electrolyte Interphase Formation. *ACS Appl. Mater. Interfaces* **2016**, *8* (19), 12211−12220.

(11) Hays, K. A.; Ruther, R. E.; Kukay, A. J.; Cao, P.; Saito, T.; Wood, D. L.; Li, J. What Makes Lithium Substituted Polyacrylic Acid a Better Binder than Polyacrylic Acid for Silicon-Graphite Composite Anodes? *J. Power Sources* **2018**, *384*, 136−144.

(12) Son, S.-B.; Wang, Y.; Xu, J.; Li, X.; Groner, M.; Stokes, A.; Yang, Y.; Cheng, Y.-T.; Ban, C. Systematic Investigation of the Alucone-Coating Enhancement on Silicon Anodes. *ACS Appl. Mater. Interfaces* **2017**, *9* (46), 40143−40150.

(13) Piper, D. M.; Travis, J. J.; Young, M.; Son, S.-B.; Kim, S. C.; Oh, K. H.; George, S. M.; Ban, C.; Lee, S.-H. Reversible High-Capacity Si Nanocomposite Anodes for Lithium-Ion Batteries Enabled by Molecular Layer Deposition. *Adv. Mater.* **2014**, *26* (10), 1596−1601.

(14) Riley, L. A.; Cavanagh, A. S.; George, S. M.; Lee, S.-H.; Dillon, A. C. Improved Mechanical Integrity of ALD-Coated Composite Electrodes for Li-Ion Batteries. *Electrochem. Solid-State Lett.* **2011**, *14* (3), A29.

(15) Molina Piper, D.; Lee, Y.; Son, S.-B.; Evans, T.; Lin, F.; Nordlund, D.; Xiao, X.; George, S. M.; Lee, S.-H.; Ban, C. Cross-Linked Aluminum Dioxybenzene Coating for Stabilization of Silicon Electrodes. *Nano Energy* **2016**, *22*, 202−210.

(16) Ma, Y.; Martinez de la Hoz, J. M.; Angarita, I.; Berrio-Sanchez, J. M.; Benitez, L.; Seminario, J. M.; Son, S.-B.; Lee, S.-H.; George, S. M.; Ban, C.; et al. Structure and Reactivity of Alucone-Coated Films on Si and Li(x)Si(y) Surfaces. *ACS Appl. Mater. Interfaces* **2015**, *7* (22), 11948−11955.

(17) García, J. M.; García, F. C.; Serna, F.; de la Peña, J. L. High-Performance Aromatic Polyamides. *Prog. Polym. Sci.* **2010**, *35* (5), 623−686.

(18) Tashiro, K.; Kobayashi, M.; Tadokoro, H. Elastic Moduli and Molecular Structures of Several Crystalline Polymers, Including Aromatic Polyamides. *Macromolecules* **1977**, *10* (2), 413−420.

(19) Yang, H.; Wang, Y.; Duh, J.-G. Developing a Diamine-Assisted Polymerization Method To Synthesize Nano-$LiMnPO_4$ with N-Doped Carbon from Polyamides for High-Performance Li-Ion Batteries. *ACS Sustainable Chem. Eng.* **2018**, *6* (10), 13302−13311.

(20) Choi, N.-S.; Yew, K. H.; Choi, W.-U.; Kim, S.-S. Enhanced Electrochemical Properties of a Si-Based Anode Using an Electrochemically Active Polyamide Imide Binder. *J. Power Sources* **2008**, *177* (2), 590−594.

(21) Chen, J.; Liu, Q.; Wang, B.; Li, F.; Jiang, H.; Liu, K.; Wang, Y.; Li, M.; Lu, Z.; Wang, D. Hierarchical Polyamide 6 (PA6) Nanofibrous Membrane with Desired Thickness as Separator for High-Performance Lithium-Ion Batteries. *J. Electrochem. Soc.* **2017**, *164* (7), A1526−A1533.

(22) Higgs, D. J.; DuMont, J. W.; Sharma, K.; George, S. M. Spatial Molecular Layer Deposition of Polyamide Thin Films on Flexible Polymer Substrates Using a Rotating Cylinder Reactor. *J. Vac. Sci. Technol., A* **2018**, *36* (1), 01A117.

(23) Sharma, K.; Hall, R. A.; George, S. M. Spatial Atomic Layer Deposition on Flexible Substrates Using a Modular Rotating Cylinder Reactor. *J. Vac. Sci. Technol., A* **2015**, *33* (1), 01A132.

(24) Yersak, A. S.; Sharma, K.; Wallas, J. M.; Dameron, A. A.; Li, X.; Yang, Y.; Hurst, K. E.; Ban, C.; Tenent, R. C.; George, S. M. Spatial Atomic Layer Deposition for Coating Flexible Porous Li-Ion Battery Electrodes. *J. Vac. Sci. Technol., A* **2018**, *36* (1), 01A123.

(25) Oliver, W. C.; Pharr, G. M. An Improved Technique for Determining Hardness and Elastic Modulus Using Load and Displacement Sensing Indentation Experiments. *J. Mater. Res.* **1992**, *7* (06), 1564−1583.

(26) Wang, Y.; Zhang, Q.; Li, D.; Hu, J.; Xu, J.; Dang, D.; Xiao, X.; Cheng, Y.-T. Mechanical Property Evolution of Silicon Composite Electrodes Studied by Environmental Nanoindentation. *Adv. Energy Mater.* **2018**, *8* (10), 1702578.

(27) Komaba, S.; Shimomura, K.; Yabuuchi, N.; Ozeki, T.; Yui, H.; Konno, K. Study on Polymer Binders for High-Capacity SiO Negative Electrode of Li-Ion Batteries. *J. Phys. Chem. C* **2011**, *115* (27), 13487−13495.

(28) Elam, J. W.; Routkevitch, D.; Mardilovich, P. P.; George, S. M. Conformal Coating on Ultrahigh-Aspect-Ratio Nanopores of Anodic

DOI: 10.1021/acsaem.9b00326
ACS Appl. Energy Mater. 2019, 2, 4135−4143

Alumina by Atomic Layer Deposition. *Chem. Mater.* **2003**, *15* (18), 3507−3517.
(29) Yim, T.; Choi, S. J.; Jo, Y. N.; Kim, T.-H.; Kim, K. J.; Jeong, G.; Kim, Y.-J. Effect of Binder Properties on Electrochemical Performance for Silicon-Graphite Anode: Method and Application of Binder Screening. *Electrochim. Acta* **2014**, *136*, 112−120.
(30) Li, D.; Wang, Y.; Hu, J.; Lu, B.; Dang, D.; Zhang, J.; Cheng, Y.-T. Role of Polymeric Binders on Mechanical Behavior and Cracking Resistance of Silicon Composite Electrodes during Electrochemical Cycling. *J. Power Sources* **2018**, *387*, 9−15.
(31) Li, N.-W.; Yin, Y.-X.; Yang, C.-P.; Guo, Y.-G. An Artificial Solid Electrolyte Interphase Layer for Stable Lithium Metal Anodes. *Adv. Mater.* **2016**, *28* (9), 1853−1858.
(32) Lin, D.; Liu, Y.; Cui, Y. Reviving the Lithium Metal Anode for High-Energy Batteries. *Nat. Nanotechnol.* **2017**, *12* (3), 194−206.
(33) Jin, Y.; Zhu, B.; Lu, Z.; Liu, N.; Zhu, J. Challenges and Recent Progress in the Development of Si Anodes for Lithium-Ion Battery. *Adv. Energy Mater.* **2017**, *7* (23), 1700715.
(34) Ogata, K.; Jeon, S.; Ko, D.-S.; Jung, I. S.; Kim, J. H.; Ito, K.; Kubo, Y.; Takei, K.; Saito, S.; Cho, Y.-H.; et al. Evolving Affinity between Coulombic Reversibility and Hysteretic Phase Transformations in Nano-Structured Silicon-Based Lithium-Ion Batteries. *Nat. Commun.* **2018**, *9* (1), 479.
(35) McDowell, M. T.; Lee, S. W.; Nix, W. D.; Cui, Y. 25th Anniversary Article: Understanding the Lithiation of Silicon and Other Alloying Anodes for Lithium-Ion Batteries. *Adv. Mater.* **2013**, *25* (36), 4966−4985.
(36) Ban, C.; George, S. M. Molecular Layer Deposition for Surface Modification of Lithium-Ion Battery Electrodes. *Adv. Mater. Interfaces* **2016**, *3* (21), 1600762.
(37) Li, L.; Cabán-Acevedo, M.; Girard, S. N.; Jin, S. High-Purity Iron Pyrite (FeS_2) Nanowires as High-Capacity Nanostructured Cathodes for Lithium-Ion Batteries. *Nanoscale* **2014**, *6* (4), 2112−2118.
(38) Girishkumar, G.; McCloskey, B.; Luntz, A. C.; Swanson, S.; Wilcke, W. Lithium−Air Battery: Promise and Challenges. *J. Phys. Chem. Lett.* **2010**, *1* (14), 2193−2203.
(39) Yoon, T.; Nguyen, C. C.; Seo, D. M.; Lucht, B. L. Capacity Fading Mechanisms of Silicon Nanoparticle Negative Electrodes for Lithium Ion Batteries. *J. Electrochem. Soc.* **2015**, *162* (12), A2325−A2330.
(40) Varma, I. K.; Kumar, R.; Bhattacharyya, A. B. Effect of Structure on Properties of Aromatic Polyamides. *J. Appl. Polym. Sci.* **1990**, *40* (34), 531−542.
(41) Benavente, J.; De Abajo, J.; De La Campa, J. G.; Garcia, J. M. Electrical Properties of Modified Aromatic Polyamide Membranes. *Sep. Sci. Technol.* **1997**, *32* (13), 2189−2199.

DOI: 10.1021/acsaem.9b00326
ACS Appl. Energy Mater. 2019, 2, 4135−4143